Available online at www.sciencedirect.com
ScienceDirect
Developmental Biology 317 (2008) 213–224
DEVELOPMENTAL BIOLOGY
www.elsevier.com/developmentalbiology

Sox9 is required for invagination of the otic placode in mice

Francisco Barrionuevo [a,*], Angela Naumann [b], Stefan Bagheri-Fam [a,1], Volker Speth [c], Makoto M. Taketo [d], Gerd Scherer [a], Annette Neubüser [b]

[a] *Institute of Human Genetics and Anthropology, University of Freiburg, Breisacherstr. 33, D-79106 Freiburg, Germany*
[b] *Developmental Biology, Institute of Biology 1, University of Freiburg, Hauptstrasse 1, D-79104 Freiburg, Germany*
[c] *Cell Biology, Institute of Biology II, University of Freiburg, Schänzlestrasse 1, D-79104 Freiburg, Germany*
[d] *Department of Pharmacology, Graduate School of Medicine, Kyoto University, Yoshida-Konoé-cho, Sakyo-ku, Kyoto 606-8501, Japan*

Received for publication 20 December 2007; revised 7 February 2008; accepted 8 February 2008
Available online 21 February 2008

Abstract

The HMG-domain-containing transcription factor Sox9 is an important regulator of chondrogenesis, testis formation and development of several other organs. *Sox9* is expressed in the otic placodes, the primordia of the inner ear, and studies in *Xenopus* have provided evidence that *Sox9* is required for otic specification. Here we report novel and different functions of *Sox9* during mouse inner ear development. We show that in mice with a *Foxg1*^{Cre}-mediated conditional inactivation of *Sox9* in the otic ectoderm, otic placodes form and express markers of otic specification. However, mutant placodes do not attach to the neural tube, fail to invaginate, and subsequently degenerate by apoptosis, resulting in a complete loss of otic structures. Transmission-electron microscopic analysis suggests that cell–cell contacts in the *Sox9* mutant placodes are abnormal, although E-cadherin, N-cadherin, and beta-catenin protein expression are unchanged. In contrast, expression of Epha4 was downregulated in mutant placodes. In embryos with a *Keratin-19*^{Cre}-mediated mosaic inactivation of *Sox9*, Sox9-negative and Sox9-positive cells in the otic ectoderm sort out from one another. In these embryos only Sox9-positive cells invaginate and form one or several micro-vesicles, whereas Sox9-negative cells stay behind and die. Our findings demonstrate that, in contrast to *Xenopus*, *Sox9* is not required for the initial specification of the otic placode in the mouse, but instead controls adhesive properties and invagination of placodal cells in a cell-autonomous manner.
© 2008 Elsevier Inc. All rights reserved.

Keywords: Sox9; Mouse inner ear development; Otic placode; Invagination

Introduction

The vertebrate inner ear, which contains the sensory organs for hearing and balance, develops from an ectodermal placode adjacent to the posterior hindbrain. In the mouse, otic development first becomes morphologically apparent at around the four-somite stage with the thickening of the ectoderm adjacent to rhombomeres five and six. The generation of a discernable otic placode takes place by the 10-somite stage. Between the 13- and 20-somite stage the placode invaginates giving rise to the otic pit, which forms a closed vesicle by the 21- to 29-somite stage. In the anterior ventral region of the otocyst, neuronal precursor cells delaminate to give rise to the cochleovestibular ganglion that will innervate the sensory cells of the inner ear. The otic vesicle then undergoes complex morphogenetic changes that ultimately generate the architecture of the adult inner ear (Barald and Kelley, 2004; Kiernan et al., 2002, and references therein).

Transplantation studies in amphibians and birds have established that the competence to form an otic vesicle is initially widely present in the embryonic ectoderm, but progressively becomes restricted to the otic region as development proceeds (Noramly and Grainger, 2002). Development of the otic placode is thought to be induced by signals from the cranial paraxial mesoderm and the hindbrain, and members of the fibroblast growth factor (FGF) family play a central role in this induction (Phillips et al., 2001; Wright and Mansour, 2003a, b). In addition, Ladher et al. (2005) recently showed that FGF

* Corresponding author. Fax: +49 761 270 7041.
E-mail address: francisco.barrionuevo@uniklinik-freiburg.de (F. Barrionuevo).
[1] Present address: Prince Henry's Institute of Medical Research, Monash Medical Centre, Melbourne, Victoria 3168, Australia.

0012-1606/$ - see front matter © 2008 Elsevier Inc. All rights reserved.
doi:10.1016/j.ydbio.2008.02.011

signals from the endoderm also contribute to otic induction, most likely by controlling *Fgf* expression in the mesoderm. Studies in chick and mouse have also provided evidence for involvement of Wnt signaling in otic placode induction (Ladher et al., 2000; Ohyama et al., 2006), although such a role in zebrafish has been questioned (Phillips et al., 2004). Placode induction is heralded by the onset of expression of a variety of genes, including the transcription factors *Pax2*, *Pax8*, *Dlx5*, *Tbx2* and *Sox9,* which appear in the presumptive placodal ectoderm before the placode becomes morphologically distinct (Barald and Kelley, 2004; Kiernan et al., 2002; Noramly and Grainger, 2002). As the development of the ear progresses to the otic vesicle stage the expression of these and other markers becomes confined to defined regions of the otic vesicle, which give rise to specific structures of the inner ear. This refinement of the gene expression patterns is also influenced by neighboring tissues including the notochord and hindbrain (Barald and Kelley, 2004; Kiernan et al., 2002). Gene targeting experiments in the mouse have revealed essential functions of an increasing number of genes expressed in the developing ear (Barald and Kelley, 2004; Kiernan et al., 2002; Noramly and Grainger, 2002). However, the genetic control of the earliest stages of otic morphogenesis, the invagination of the otic placode and the formation of an otic vesicle, is so far poorly understood.

Sox9, a member of the SoxE subgroup of HMG-domain-containing transcription factors, is expressed in the developing inner ear in several species (Bagheri-Fam et al., 2006; Liu et al., 2003; Saint-Germain et al., 2004). In humans, heterozygous *SOX9* mutations are the cause for the skeletal malformation syndrome campomelic dysplasia, which is characterized by severe general hypoplasia of the skeleton, XY sex reversal and defects in several other organ systems including the brain, pancreas and heart (OMIM 114290). Importantly, campomelic dysplasia is frequently associated with conductive and sensorineural hearing loss, including malformations of the cochlea (Houston et al., 1983; Tokita et al., 1979). Indeed, studies in *Xenopus* and zebrafish have recently provided evidence for an essential function of *Sox9* in inner ear development. Saint-Germain et al. (2004) demonstrated that morpholino antisense oligonucleotide-mediated depletion of Sox9 protein in *Xenopus* embryos resulted in loss of early otic markers and failure of otic vesicle development. They also showed that a hormone-inducible dominant negative version of Sox9 blocked otic development during gastrulation, but had little effect on otic development at later stages, indicating that Sox9 is required for otic placode specification, but not for subsequent stages of otic development. Furthermore, loss of *Sox9a* and *Sox9b* function in zebrafish resulted in a complete absence or severe reduction of the otic vesicle (Liu et al., 2003; Yan et al., 2005). In addition to these loss-of-function studies, Taylor and Labonne (2005) recently showed that over-expression of Sox9 in *Xenopus* can result in enlarged or ectopic otic vesicles.

In the mouse, the function of *Sox9* in otic development has so far not been examined. Here we used conditional gene targeting to inactivate *Sox9* in the entire prospective otic placode or only in part of its cells. In contrast to what would have been expected based on its functions in *Xenopus*, we find that in mouse *Sox9* is not essential for the initial otic specification and formation of a morphologically recognizable otic placode. Instead, we show that Sox9 is cell-autonomously required for placode invagination, and we provide evidence that *Sox9* controls adhesive properties of placodal cells and regulates *Epha4* expression.

Materials and methods

Mice

$Sox9^{flox/flox}$ mice (Kist et al., 2002) were bred to $Foxg1^{Cre}$ mice (Hebert and McConnell, 2000) in a mixed background. $Foxg1^{Cre};Sox9^{flox/+}$ mice were viable and fertile and were backcrossed to $Sox9^{flox/flox}$ mice to obtain $Foxg1^{Cre};Sox9^{flox/flox}$ embryos. Generation of $K19^{Cre};Sox9^{flox/flox}$ mice has been previously described (Barrionuevo et al., 2006). For timed pregnancies, plugs were checked in the morning after mating, noon was taken as embryonic day (E) 0.5. Genotyping was carried out on genomic DNA derived from adult tails or embryonic yolk sacs using established PCR protocols for the *Cre* allele (Lecureuil et al., 2002) and for the *Sox9* and $Sox9^{flox}$ alleles (Kist et al., 2002).

Histology, RNA in situ hybridization, immunostaining and electron microscopy

For whole mount RNA in situ hybridization, embryos were fixed, processed and hybridized as described by Henrique et al. (1995). cDNAs used to generate riboprobes for *Pax2*, *Pax8* (Dorfler and Busslinger, 1996), *Dlx5* (Liu et al., 1997), *Sox8* (Sock et al., 2001), *Sox10* (Kuhlbrodt et al., 1998), *Tbx2* (Chapman et al., 1996), *Pea3* (Taylor et al., 1997), *NeuroD* (Gradwohl et al., 2000), *Fgf3* (Mansour and Martin, 1988), *Epha4* (Mori et al., 1995) and *Col2a1* (Rahkonen et al., 2003) are described in the cited references. To generate a probe for *Erm*, a 674 bp fragment was amplified by RT-PCR from mouse embryo cDNA using the primers Erm5′ (TTG GTG CTT CAT GCT CCA CC) and Erm3′ (GTC AGC ACA GTA ATC TCG GG) and cloned into pCRII-TOPO (Invitrogen). Embryos for histological analyses were collected in PBS, fixed in Serra (ethanol/37% formaldehyde/acetic acid, 6:3:1), embedded in paraffin, sectioned at 7 μm and stained with hematoxylin and eosin. Immunostaining was performed using the Peroxidase Vectastain ABC Kit (Vector Laboratories) following the manufacturer's instructions. For immunofluorescence we used Alexa Fluor 594 rabbit anti-goat IgG (1:150), biotinylated secondary antibodies (Vector Laboratories) or the M.O.M kit (Vector Laboratories) and the Fluorescent Avidin Kit (Vector Laboratories) following the manufacturer's instructions. Primary antibodies used were: rabbit anti-Sox9 (gift of M. Wegner, Stolt et al. 2003, 1:200), goat anti-Sox9 (Santa Cruz; sc-17341; 1:50), mouse anti-N-Cadherin (BD Biosciences, Cat# 610920, 1:100), mouse anti-E-Cadherin (BD Biosciences, Cat# 610404, 1:100), mouse anti-beta-Catenin (BD Biosciences, Cat# 610154, 1:100), rabbit anti-N-CAM (Chemicon, Cat# AB5032, 1:100), rabbit anti-Pax2 (Covance, Cat# PRB-276P, 1:100) and goat anti-EphA4 (R&D, Cat# AF641; 1:100). For fluorescence counterstaining of nuclei, DAPI (4′,6-diamidino-2-phenylindole, Molecular Probes, 100 ng/ml in PBS) was used. Detailed staining protocols are available upon request. Confocal images were captured using a Zeiss LSM 510 laser scanning microscope.

For whole mount immunohistochemistry, embryos were collected in PBS, fixed in methanol:dimethyl sulfoxide (4:1) and processed as described (Nagy et al., 2003) using a 1:200 dilution of the rabbit anti-Sox9 antibody.

For electron microscopy, embryos were fixed in buffered 2.5% glutaraldehyde and 2% osmiumtetroxide, and embedded in Epon 812 resin. Ultra-thin sections were stained with uranyl acetate and lead citrate and examined in a Philips CM 10 electron microscope, equipped with a Gatan Bio-scan camera Model 792.

Analysis of cell proliferation and cell death

For cell proliferation, 7 μm sections were stained with an anti-phosphohistone H3 antibody (Upstate, Cat# 06-570, 1:200) as described (http://www.ihcworld.com/_protocols/antibody_protocols/histone_h3_upstate.htm), and

counterstained with hematoxylin. The number of labeled cells as well as total cell numbers per otic placode was scored.

Detection of apoptotic cells in paraffin sections was performed using either the In Situ Cell Death Detection Kit (Roche) following the producer's guidelines or using a rabbit anti-Caspase3-active antibody (R&D Systems, Cat# AF-835) as described (http://www.ihcworld.com/_protocols/antibody_protocols/caspase3_r&d_system.htm), but using a 1:100 dilution and the Fluorescent Avidin Kit (Vector Laboratories) to perform immunofluorescence detection.

Results

Tissue specific inactivation of Sox9 in the early otic ectoderm

It has previously been shown that *Foxg1*^{Cre} drives Cre activity into the prospective otic ectoderm and leads to complete recombination of floxed transgenes in the otocyst (Hebert and McConnell, 2000; Pirvola et al., 2002). In order to generate embryos with a conditional inactivation of *Sox9* in the developing inner ear, we therefore crossed mice with a floxed allele of *Sox9* (*Sox9*^{flox}; Kist et al., 2002) to mice carrying *Foxg1*^{Cre} to generate *Sox9*$^{flox/flox}$;*Foxg1*^{Cre} embryos.

Hebert and McConnell (2000) have shown that the genetic background and the loxP target loci both influence the recombination pattern obtained with Foxg1-Cre. We therefore first examined whether Foxg1-Cre mediated recombination leads to a complete loss of *Sox9* expression, and whether recombination occurs before or after the onset of Sox9-expression. In *Sox9*$^{flox/+}$, *Sox9*$^{flox/flox}$, or *Sox9*$^{flox/+}$;*Foxg1*^{Cre} embryos (hereafter referred to as control embryos), the first Sox9-positive cells can be detected in the prospective otic area at the four- to five-somite stage (Figs. 1a, c). By the eight-somite stage, Sox9 is expressed in a large proportion of the cells in the otic region, and by the 10-somite stage, the entire nascent otic placode is Sox9 positive (Figs. 1e, g, i, k, dashed circle). In *Sox9*$^{flox/flox}$;*Foxg1*^{Cre} embryos (hereafter referred to as *Sox9* mutant embryos), no Sox9-positive cells were detectable in the same region at the 10-somite stage or any later stage (Figs. 1h, j, l, dashed circle, and data not shown). In a small proportion of *Sox9* mutant embryos less than 10 *Sox9*-positive cells were transiently detectable at the eight-somite stage (Fig. 1f, small arrows), indicating that *Foxg1-Cre*-mediated recombination of *Sox9* largely occurs prior to the onset of *Sox9* expression and that in mutant embryos the vast majority of cells in the otic region never express *Sox9*.

Otic placodes are specified in the absence of Sox9 in mice

Recent studies in *Xenopus* and zebrafish have provided evidence for an essential function of *Sox9* in otic placode specification (Liu et al., 2003; Saint-Germain et al., 2004). To see whether *Sox9* is required for otic specification also in mice, we examined the otic region in mutant and control embryos at the 10–12 somite stage. Hematoxylin/Eosin-stained sections revealed a thickening of the ectoderm adjacent to the hindbrain in the presumptive otic region in both control and mutant embryos (Figs. 2a, a′, b). To further address otic specification of the thickened ectoderm, we analyzed the expression of markers of early otic development. FGF signaling is essential for otic placode induction but also plays important roles at later stages of otic development. Expression of the Ets-domain transcription factor genes *Erm* and *Pea3* is dependent on FGF signaling in many areas of the early embryo and can thus be used as a reporter for FGF signaling activity (Firnberg and Neubuser, 2002; Raible and Brand, 2001; Roehl and Nusslein-Volhard, 2001). Both genes were expressed in the otic region of mutant embryos in patterns similar to control embryos, indicating that FGF signaling is not affected by the absence of Sox9 (Figs. 2c,

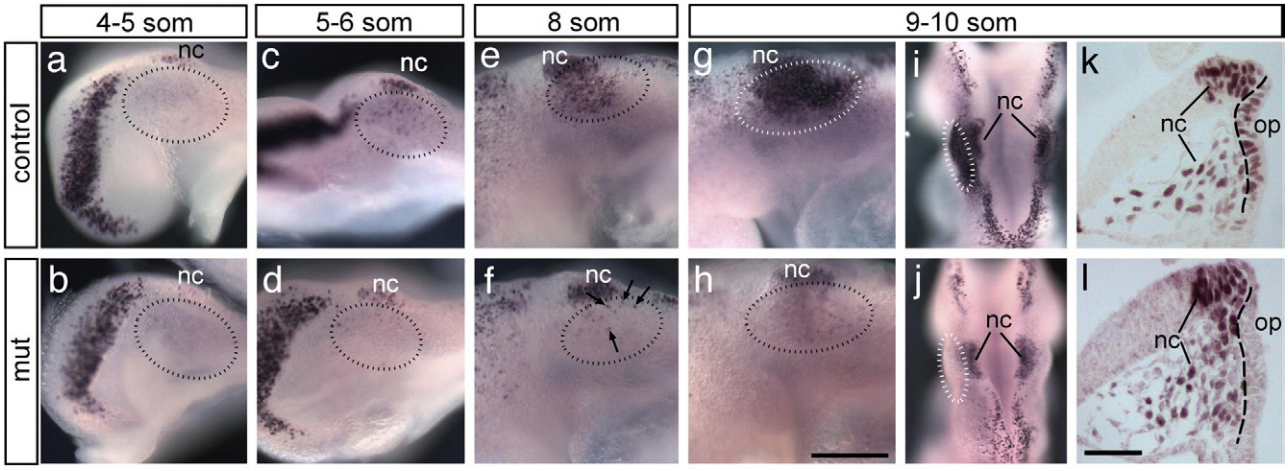

Fig. 1. Recombination takes place before the onset of *Sox9* expression in *Sox9*$^{flox/flox}$;*Foxg1*^{Cre} embryos. (a–h) Sox9 whole mount immunohistochemistry in control and *Sox9* mutant (mut) embryos. Dashed circles indicate the otic region. In controls, Sox9-positive cells are first detected at the 5–6-somite stage (c), and increase in number at subsequent stages (e, g). At the same stages, the otic region of *Sox9* mutants is largely devoid of Sox9-positive cells. A few Sox9-positive cells can transiently be detected at the 8-somite stage (f, small arrows). Panels i, j show dorsal views of the embryos shown in panels g and h to indicate that the diffuse staining visible in the dashed circle in the mutant embryo shown in panel h is not localized in the otic ectoderm. (k, l) Sox9 immunohistochemistry on sections through the otic placode of 10-somite stage mutant and control embryos confirms that the mutant otic placode is devoid of Sox9 positive cells, but that Sox9 staining is detectable in neural crest cells beneath the placode. This staining in neural crest cells is responsible for the diffuse staining visible in panel h. (nc) Sox9-positive neural crest cells, (op) otic placode; the scale bar in panel h corresponds to 150 μm in panels a–h and to 250 μm in panels i, j; the scale bar in panel l corresponds to 50 μm in panels k, l.

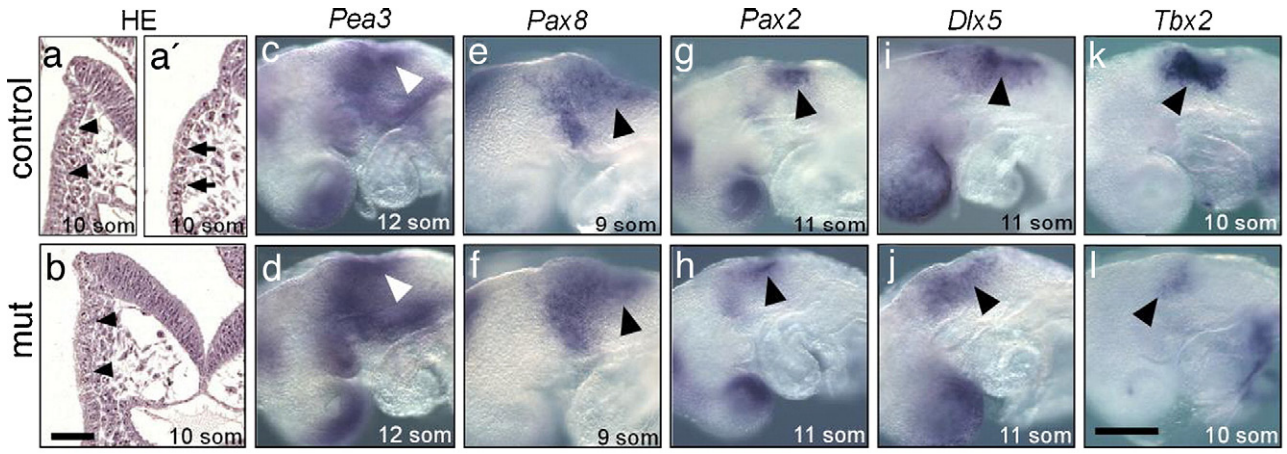

Fig. 2. Otic specification occurs in the absence of Sox9. (a, b) Hematoxylin/eosin-stained transverse sections through the otic region of control and *Sox9* mutant (mut) embryos at the 10-somite stage reveal a thickening of the ectoderm in both embryos (arrowheads). Panel a′ shows a hematoxylin/eosin-stained section through the same embryo as in panel a but at a level posterior to the otic region to show the thickness of non-otic head ectoderm (arrows) for comparison. (c–j) Whole mount in situ hybridizations with the indicated probes and at the indicated stages show similar expression of markers of otic specification in mutant and control embryos. (k, l) Expression of *Tbx2* in the otic ectoderm is reduced in the absence of Sox9. In panels c–l, anterior is to the left, arrowheads label the otic placode. The scale bar in panel b corresponds to 50 μm in panels a, a′, b; the scale bar in panel l corresponds to 400 μm in panels c–l.

d, Figs. S1a, b). The transcription factors *Pax8*, *Pax2* and *Dlx5* are markers of otic specification and are essential for later stages of inner ear development (Noramly and Grainger, 2002, and references therein). At the 9- to 11-somite stage, no difference in expression of *Pax8*, *Pax2* and *Dlx5* was detectable in mutant and control otic ectoderm (Figs. 2e–j, Figs. S1c–f). Expression of the transcription factor *Tbx2* is also initiated during otic specification shortly after the onset of Sox9 protein expression (Fig. 2k, Fig. S2). Its function during inner ear development, however, has not yet been analyzed. In contrast to *Pax8*, *Pax2* and *Dlx5*, expression of *Tbx2* in mutant embryos was reduced and confined to a smaller domain at all stages analyzed (Fig. 2l, Figs. S1g, h). Together, these analyses indicate that a morphologically distinct otic placode expressing markers of otic specification can form in the absence of Sox9. However, Sox9 is already required at this early stage for the initiation of normal *Tbx2* expression.

Sox9 is necessary for otic placode invagination

To follow the development of the inner ear in the absence of Sox9, we first examined mutant embryos at E9.5 and E11.5. At E9.5, a small otic placode that had failed to invaginate was present instead of the otic vesicle found in control littermates (Figs. 3a, b), and by E11.5, mutants lacked all inner ear structures (Figs. 1c, d). This finding suggests that otic development is initiated in the absence of *Sox9*, but that otic structures degenerate at later stages. To determine when phenotypic differences between mutant and control embryos can first be detected, we examined Hematoxylin/Eosin-stained sections of the otic region between E8.0 (10-somite stage) and E9.5 (22-somite stage). At the 10-somite stage, the otic region in both mutant and control embryos is covered by a thickened ectoderm, which forms a morphologically distinct placode by the 13-somite stage (Figs. 3e, f). At this stage in control embryos, the placode starts to invaginate to form the otic pit (Fig. 3e). Invagination is more pronounced at the 15- and 18-somite stages (Figs. 3g, i), and an otic vesicle forms by the 22-somite stage (Fig. 3k). In mutant embryos, the initial thickening of the ectoderm and the formation of a placode is normal, but placode invagination is impaired; from the 18-somite stage on, mutant placodes are also smaller than control placodes (Figs. 3f, h, j, l).

To assess whether the failure of *Sox9* mutant placodes to invaginate is an indirect consequence of the failure to maintain placode specific gene expression, we next analyzed the expression of *Pax2*, *Pax8*, *Dlx5, Erm*, *Pea3* and *Tbx2* during the process of placode invagination. At the 15- to 17-somite stage, expression of *Pax2*, *Dlx5,* and *Pea3* was maintained in the non-invaginating *Sox9* mutant placodes at levels similar to those in control placodes (Figs. 3m–r). The same expression patterns were observed for *Pax8* and *Erm* (not shown). Similar to the earlier stage, *Tbx2* expression was reduced in mutant placodes (Figs. 3s, t). Thus, the failure of mutant otic placodes to invaginate seems not to be caused by a loss of otic specification.

To see whether any neuronal precursors for the vestibular cochlear ganglion are specified in the absence of Sox9, we compared the expression of *NeuroD* and *Fgf3* in mutant and control embryos. This analysis suggests that the first neuronal precursors for the acoustic ganglion are specified in the absence of Sox9. However, these cells are subsequently lost in most mutants (Fig. S3).

Sox9 controls adhesive properties of placodal cells

The molecular mechanism of otic placode invagination is poorly understood and may not be dependent on changes in the actin cytoskeleton as in other invaginating tissues. Instead, normal otic placode invagination has been suggested to depend on an attachment of the placode to the hindbrain (Visconti and Hilfer, 2002). Such a close association of the dorso-medial part of the placode with the adjacent brain tissue is clearly visible in

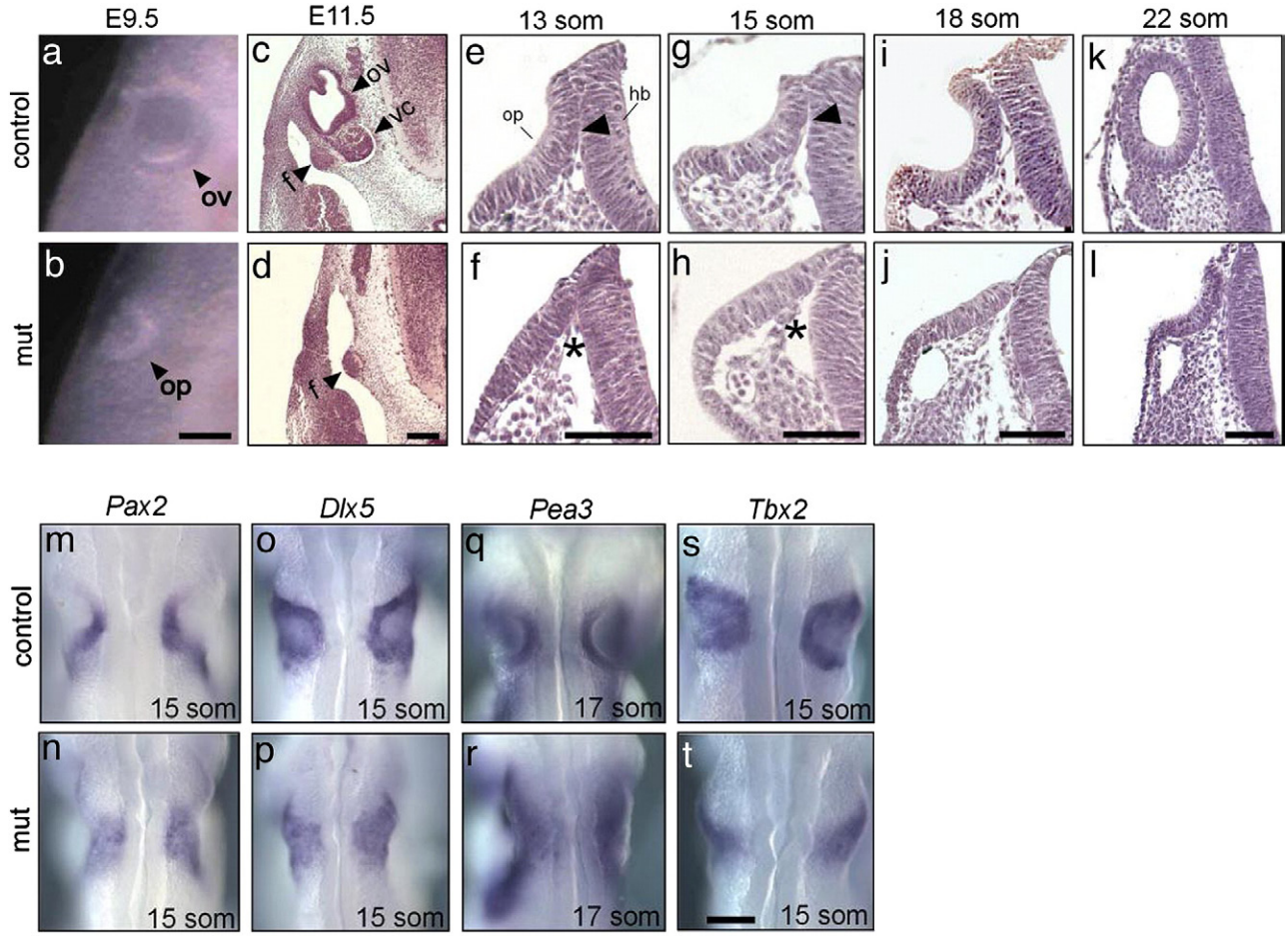

Fig. 3. *Foxg1-Cre*-mediated recombination of *Sox9* blocks otic vesicle formation despite continuous expression of markers of otic specification, and results in loss of otic structures. (a, b) Whole mount view of the otic primordium of control and *Sox9* mutant embryos at E9.5. Note that an otic vesicle has formed in the control embryo, whereas otic development is arrested at the placode stage in the *Sox9* mutant. (c, d) Hematoxylin/eosin-stained sections through the otic region of control and *Sox9* mutant embryos at E11.5. Note the complete absence of otic structures in the mutant. (e–l) Hematoxylin/eosin-stained sections through the otic region of control and *Sox9* mutant (mut) embryos at the 13- to 22-somite stage (E8.5 to E9.0) reveal a failure of Sox9 mutant placodes to invaginate. Arrowheads in panels e and g indicate association between the otic placode and the hindbrain, asterisks in panels f and h the absence of this association in mutants. (m–t) Whole mount in situ hybridizations with the indicated probes and at the indicated stages. Except for *Tbx2*, patterns in mutant embryos resemble the patterns in control embryos prior to otic placode invagination. (f) facial (geniculate) ganglion; (hb) hindbrain; (op) otic placode; (ov) otic vesicle; (som) somites; (vc) vestibular cochlear ganglion. The scale bars in panels a–l correspond to 100 μm. the scale bar in panel t corresponds to 200 μm in panels m–t.

control embryos (Figs. 3e, g, arrowheads) but is absent in *Sox9* mutants (Figs. 3f, h, asterisks). Perturbation of the extracellular matrix including the application of blocking antibodies against laminin, a component of the basement membrane, can prevent the association of the otic primordium and the hindbrain, inhibiting subsequent placode invagination (Visconti and Hilfer, 2002). To assay for changes in the basal lamina, we performed laminin immunohistochemistry in control and mutant embryos but could not detect any differences (Figs. 4a, b). To further assess the integrity of the basal lamina, we examined mutant and control placodes by transmission electron microscopy, but again could not detect any differences in the appearance of the basal lamina (Figs. 4c, d, and insets). However, we detected major differences in the structure of the placodal epithelium itself. In control placodes at both the 14- and the 17-somite stage, cells are tightly packed and very few intercellular spaces are visible (Figs. 4e, g). In contrast, the mutant epithelium appears disorganized and contains numerous intercellular spaces, in particular in the basal half of the epithelium (Figs. 4f, h). The disorganized epithelial structure was consistently seen in all six mutant placodes analyzed and absent from the six control placodes studied. Higher magnification reveals that adjacent cells contact each other over extended areas in control placodes, while contacts between neighboring cells in mutant placodes are restricted to focal areas (Figs. 4i, j, and insets). Together, these results indicate that *Sox9* controls adhesive properties of placodal cells.

We therefore next compared the expression of adhesion molecules in control and mutant placodes by immunofluorescence, using antibodies directed against E-cadherin, N-cadherin, beta-catenin and NCAM. Of these, strong NCAM staining was detected in the neural tube, notochord, and somites, but only weak staining close to background levels was detected in the otic placode or early otic vesicle, and this staining was similar in mutant and controls (Figs. S4g, h, and data not shown). For E-cadherin, N-cadherin, and beta-catenin

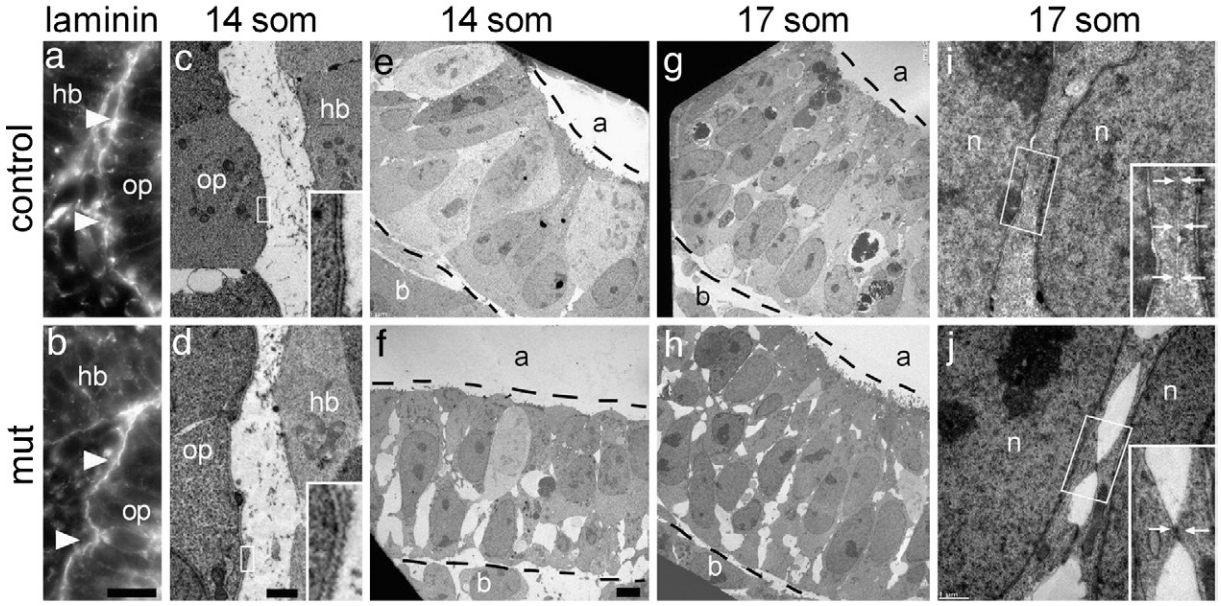

Fig. 4. Reduced cell–cell contacts in *Sox9* mutant placodes. (a, b) Antibody staining against laminin reveals the presence of a basal lamina (arrowheads) on the basal side of control and mutant placodes. (c–j) Transmission electron microscopic pictures of sections through otic placode at the 14- and 17-somite stage. (c, d) show the basal side of the otic placode of a 14-somite mutant and wildtype embryo. The insets show high magnification of the boxed regions to reveal the basal lamina. (e–h) In control placodes, the cells are tightly packed, whereas in mutant placodes at the 14- and 17-somite stage, many intercellular spaces are visible and contacts between neighboring cells are restricted to small focal areas. Dashed lines indicate the apical (a) and basal (b) limits of the placodes. (i, j) High magnification of a typical contact zone of two placode cells. Cells in control embryos contact each other over an extended area (i), while contacts between mutant cells are focal and interrupted by regions of no contact (j). Insets show a higher magnification to further demonstrate this difference. Arrows label the cell membranes that are in contact. (hb) hindbrain; (n) nucleus; (op) otic placode. The scale bar in panel b corresponds to 25 μm in panels a, b, the scale bar in panel d to 1 μm (c, d, i, j), and the scale bar in panel f to 5 μm (e–h).

we detected strong membrane associated staining in the otic placode, but we were unable to detect any difference between mutant and control placodes (Figs. S4a–f). In contrast, analysis of protein and RNA expression of the transmembrane receptor Epha4 revealed a downregulation, but not a complete loss, in mutant placodes. This downregulation was pronounced on the protein level but was also detectable on the mRNA level at the 16 somite stage (Figs. 5c–f). In particular, the apical accumulation of EphA4 protein observed in control placodes was completely missing in mutant placodes (Figs. 5e, f).

Col2a1 encodes type II collagen, a major component of the vitreous and cartilage extracellular matrix, and is regulated by *Sox9* in chondrogenesis (de Crombrugghe et al., 2000; Lefebvre et al., 1997). *Col2a1* expression was lost from Sox9 mutant placodes (Figs. 5g, h), indicating that loss of Sox9 may also affect the extracellular matrix around the developing ear placode in addition to affecting cell–cell contacts.

Sox9 mutant placode cells undergo apoptosis

Since *Sox9* mutants appear to lose *NeuroD*-positive cells at E9.5 and lack all inner ear structures at E11.5, we next examined whether the mutant otic placodes may degenerate via apoptosis. Immunostaining using antibody against activated Caspase3 and TUNEL assays (not shown) revealed no increase in apoptosis at the 14- to 16-somite stage (not shown), but a high number of apoptotic cells was present throughout the mutant otic placodes at the 18–22-somite stage (Fig. 6b). At the same stage no or only single Caspase3-positive cells at the edge of the placode were detectable in control embryos (Fig. 6a). In contrast, analysis of cell proliferation between the 15- and 17-somite stage revealed no significant differences between control and mutant placodes (Fig. 6c). Therefore, the size difference between control and mutant placodes and the eventual loss of otic tissue in mutant embryos seems to be caused by increased apoptosis.

Sox9 is necessary for Sox10 expression in the otic placode

Previous studies have shown that the three members of the *SoxE* subfamily of *Sox* genes, *Sox8*, *Sox9* and *Sox10*, can function redundantly in regions of co-expression, but also show cross-regulation (Chaboissier et al., 2004; Stolt et al., 2004; Taylor and Labonne, 2005). Both *Sox8* and *Sox10* have been reported to be expressed in the otic vesicle in the mouse at E9.5 and E10.5, respectively (Britsch et al., 2001; Sock et al., 2001). The onset of expression of these two genes in the mouse otic region, however, has not yet been analyzed. In *Xenopus*, *Sox10* expression in the developing otic placode is initiated after *Sox9* expression (Taylor and Labonne, 2005). To see whether the loss of Sox9 affects expression of *Sox8* and *Sox10*, and to evaluate whether Sox8 and Sox10 might partially compensate for the loss of Sox9 during otic placode development, we analyzed expression of *Sox8* and *Sox10* in *Sox9* mutant and control embryos. In control embryos, weak expression of *Sox10* in the developing otic placode can first be detected around the 13-somite stage, and increases in strength by the 15-somite stage (Figs. 7a, c). In *Sox9* mutants, no *Sox10* expression in the otic

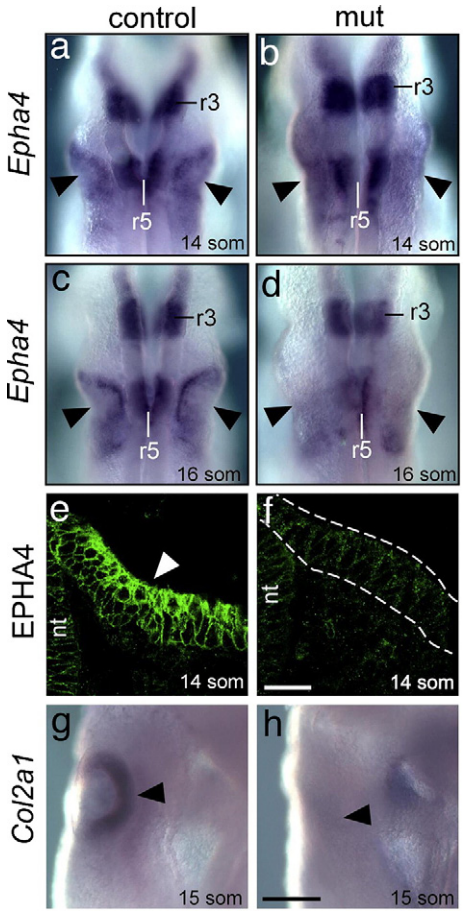

Fig. 5. Epha4 and *Col2a1* expression is downregulated in *Sox9* mutant placodes. (a–d) Whole mount in situ hybridization with an *Epha4* probe reveals a slightly weaker and less defined *Epha4* expression in mutant placodes at the 14 somite stage (a, b), and a strong reduction at the 16 somite stage (c, d). (e, f) Anti-Epha4 immunofluorescence on sections through the otic placode reveals robust membrane associated staining in control placodes and only weak staining in mutant placodes. The mutant placode in panel f is outlined with a dashed line. (g, h) Whole mount in situ hybridization with a *Col2a1* probe. *Col2a1* expression can not be detected in mutant placodes at the 15-somite stage. Arrowheads label the position of the otic placode. (nt) labels the neural tube, r3 and r5 label rhombomers-3 and -5, respectively. The scale bar in (h) corresponds to 250 μm in panels a–d, and 200 μm in panels g, h; the scale bar in panel f to 50 μm in panels e, f.

region is detectable at these stages (Figs. 7b, d). Thus, as in *Xenopus*, *Sox10* expression is initiated later than *Sox9* expression in the mouse, and is dependent on Sox9 function. We were unable to detect any *Sox8* expression in the developing otic placode above background level by in situ hybridization or immunofluorescence at E8.5 (data not shown). Together, these results rule out the possibility that functional redundancy between *SoxE* genes masks any of the functions of *Sox9* in early inner ear development in *Sox9* mutants.

Sox9 is cell-autonomously required for otic development

To address whether *Sox9* is cell-autonomously required for otic development, we used *Keratin19*^{Cre} (*K19*^{Cre}) mice which drive *Cre* expression in a mosaic pattern throughout the

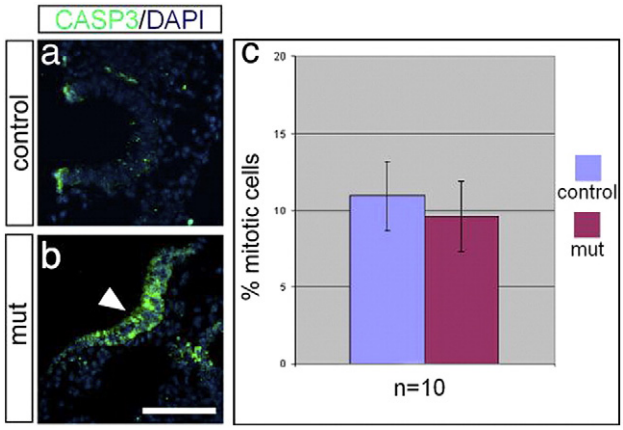

Fig. 6. *Sox9* mutant placodes disappear by apoptosis. (a, b) Antibody staining against activated Caspase3 (green) on sections through the otic region shows a significant increase in the number of apoptotic cells in *Sox9* mutant placodes (arrowhead). The sections are counterstained with DAPI to label the nuclei. (Representative examples of serial sections through three mutant and control embryos are shown.) (c) Antibody staining against phospho-histone H3 reveals no significant difference between the percentage of mitotic cells in mutant and control placodes at the 15–17-somite stage ($n=10$, number of placodes analyzed for each genotype). The scale bar in panel b corresponds to 100 μm in panels a, b.

epiblast, resulting in recombination of floxed transgenes in 20–100% of all epiblast cells at E5.5 (Means et al., 2005). Analysis of *Sox9*$^{flox/flox}$;*K19*$^{Cre/+}$ embryos (hereafter referred to as *Sox9* mosaic embryos) at E9.5 revealed the presence of one or several micro-vesicles in the otic area (Figs. 8Aa, b). Occasionally, vesicles of almost normal size were also observed. Interestingly, both micro-vesicles and larger vesicles are entirely formed by Sox9-positive cells (Figs. 8Ac–f). At E8.5–E8.75 (10- to 15-somite stage), the otic placodes of *Sox9* mosaic embryos contain individual Sox9-positive cells, or clusters of such cells (Figs. 8Ba–d), which invaginate to form micro-vesicles at E9.25 (Figs. 8Be, f). Occasionally, individual Sox9-positive cells, which apparently had failed to associate with an

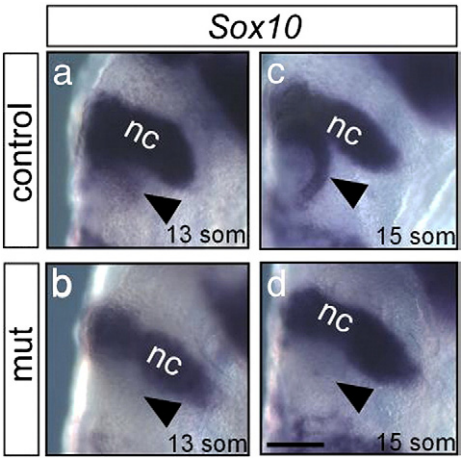

Fig. 7. *Sox10* is not expressed in *Sox9* mutant otic placodes. (a–d) Whole mount in situ hybridization of control (a, c) and *Sox9* mutant (b, d) embryos with a *Sox10* probe at the 13- (a, b) and 15-somite (c, d) stage. Arrowheads label the otic placode. (nc) labels *Sox10* expression in neural crest cells. The scale bar in panel d corresponds to 200 μm in panels a–d.

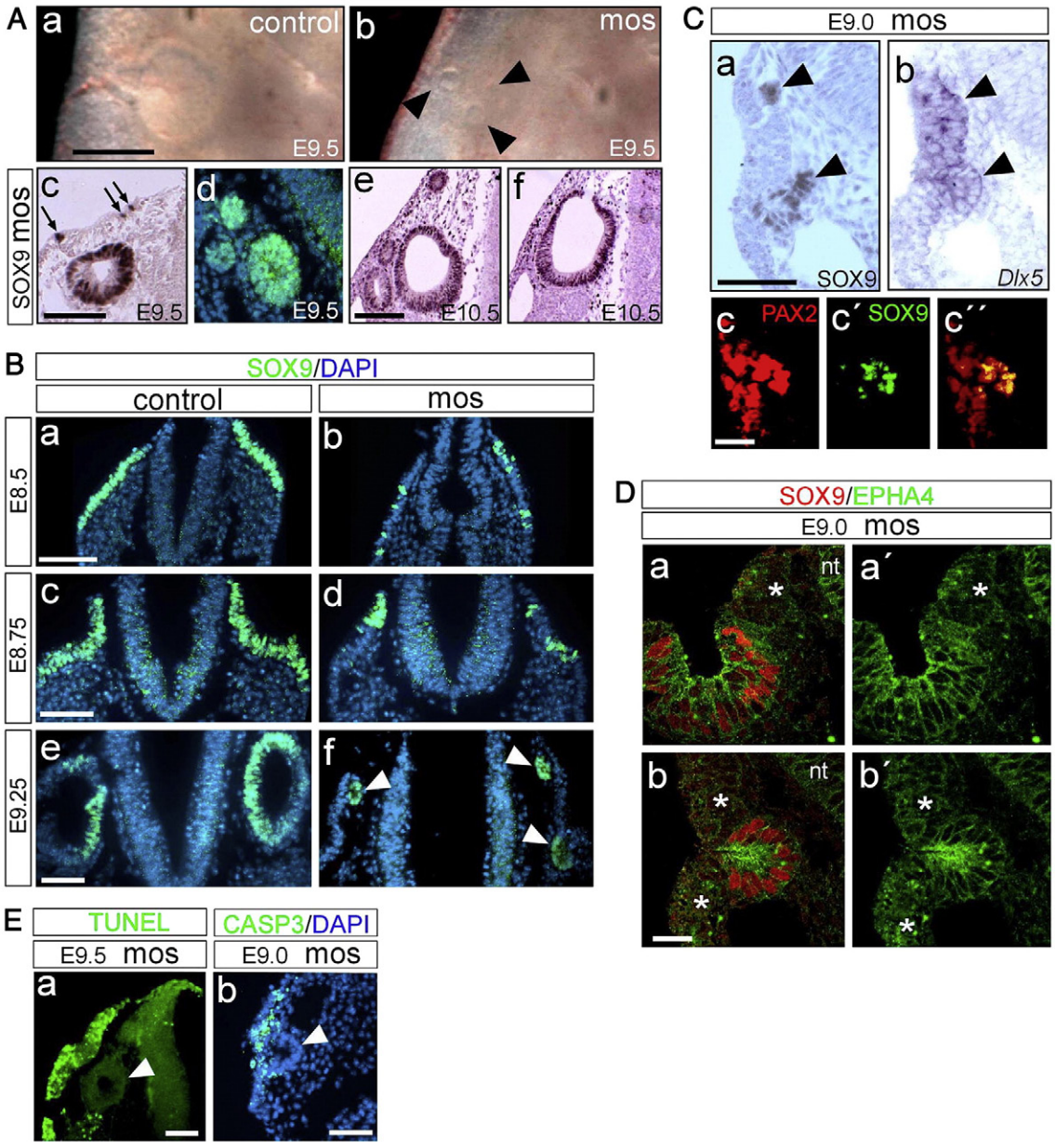

Fig. 8. Phenotype of *Sox9* mosaic embryos. (A) *Sox9* mosaic embryos form one or several small Sox9-positive otic vesicles. (Aa, b) Whole mount view of the otic region of a control and *Sox9* mosaic (mos) embryo at E9.5. Arrowheads label the otic vesicles. (Ac–f) Sections through the otic region of *Sox9* mosaic embryos at E9.5 and E10.5, stained with a Sox9-specific antibody. Small arrows in panel c label individual Sox9-positive cells among Sox9-negative non-invaginating placode cells. (B) Sox9 immunofluorescence on sections through the otic region of E8.5 to E9.25 control (Ba, c, e) and Sox9 mosaic (Bb, d, f) embryos. Arrowheads in panel f label invaginating clusters of Sox9-positive cells. (C) Sox9-positive and -negative cells in E9.0 *Sox9* mosaic placodes express *Dlx5* and *Pax2*, but only Sox9-positive cells invaginate. (Ca) Sox9 immunohistochemistry, (Cb) *Dlx5* in situ hybridization on a neighboring section to the section in panel Ca. Arrowheads label invaginating Sox9-positive cell clusters. (Cc–c″) Double-immunofluorescence against Pax2 (c, red) and Sox9 (c′, green) and overlay (c″). (D) Double-immunofluorescence against Epha4 (green) and Sox9 (red). (a, b) Overlays, (a′, b′) detection of Epha4 only. Asterisks label Sox9 negative regions of the placodes. (nt), neural tube. (E) Non-invaginating, Sox9-negative cells in the placode die by apoptosis. TUNEL assay (Ea) and anti-activated Caspase3 immunofluorescence (Eb) on sections through the otic region of *Sox9* mosaic embryos. Note that no cell death is detected in the formed otic vesicle (Ea, arrowhead) or invaginating part of the placode (Eb, arrowhead). The sections shown in panels Ad, B, Eb) were counterstained with DAPI (blue) to label the nuclei. The scale bars in panels A, B, Ca, b, E) correspond to 100 μm, and to 20 μm in panels Cc′–c″, D).

invaginating cluster of Sox9-positive cells, were still detectable among the Sox9-negative cells at E9.5 (Fig. 8Ac, arrows). Both Sox9-positive and Sox9-negative cells in the mosaic otic placode express the otic markers *Dlx5* and *Pax2* (Fig. 8C). However, only Pax2/Sox9-double positive cells of the placode invaginate (Figs. 8Cc–c″). Invaginating Sox9-positive clusters of cells show a higher level of Epha4 staining and a strong accumulation of the protein on the apical side of cells which is missing from Sox9-negative regions of the placode (Fig. 8D). TUNEL assays and immunostaining for activated Caspase3 show that the Sox9-negative cells in the mosaic placode subsequently initiate apoptosis (Fig. 8E), similar to what is

observed after complete inactivation of *Sox9* in all cells of the placode (Figs. 6b, d). This analysis of *Sox9* mosaic embryos shows that *Sox9* is cell-autonomously required for the invagination of placodal cells.

Discussion

To address the role of *Sox9* in the development of the murine inner ear, we have conditionally inactivated *Sox9* in the prospective otic region using mice with a $Foxg1^{Cre}$ allele. This approach reveals novel functions of Sox9 in inner ear development in the mouse. In the absence of Sox9, otic placodes form, but the adhesive properties of the placodal cells are severely compromised and expression of the transmembrane receptor Epha4 is downregulated. Subsequently, mutant placodes fail to invaginate and degenerate by apoptosis. By means of a second Cre line harboring the $K19^{Cre}$ allele we have created embryos with a mosaic recombination of *Sox9* in the otic region. In these embryos, only Sox9-positive cells invaginate, indicating that Sox9 is cell-autonomously required for the invagination of otic placode cells.

Sox9 is necessary for otic placode invagination in mice

Our finding that *Sox9* is absolutely required for otic placode invagination and otic vesicle formation suggests a key function of Sox9 in this process. In the absence of *Sox9*, the otic placode is formed but fails to invaginate, even though *Pax2*, *Pax8* and *Dlx5*, markers of otic specification, continue to be expressed. The failure of otic vesicle formation is thus not a secondary consequence of a failure to maintain otic specification in the absence of Sox9.

The molecular mechanism of otic placode invagination is poorly understood. Previous studies manipulating ATP levels or disrupting Ca^{2+} transport, conditions that interfere with the interaction of cytoskeletal actin and myosin, revealed no effect on otic placode invagination (Hilfer et al., 1989). It was therefore suggested that otic placode invagination may not be dependent on the formation of a contractile actin ring as in other invaginating tissues (Pilot and Lecuit, 2005). Instead, it has been proposed that normal otic placode invagination requires attachment of the placode to the hindbrain (Visconti and Hilfer, 2002). In support of this idea, perturbation of the extracellular matrix by injecting blocking antibodies against laminin or heparansulfate proteoglycans into chick embryos prevented the association of the otic primordium and the hindbrain and inhibited subsequent placode invagination (Moro-Balbas et al., 2000; Visconti and Hilfer, 2002). However, other studies had shown that otic placodes isolated from 10-somite stage quail embryos and transplanted to the lateral trunk of chick hosts form otic vesicles at very high frequency even though they are positioned far away from the neural tube (Groves and Bronner-Fraser, 2000). The importance of association of the otic placode with the hindbrain for invagination and vesicle formation in avian embryos is thus currently unclear.

Even less is known in the mouse. The analysis of *Gata3* mutants provided evidence that otic vesicle formation can occur even when contact of the otic placode with the neural tube is reduced (Lillevali et al., 2006). We detected a close association of the dorso-medial part of the placode with the adjacent brain tissue in control mouse embryos, which is absent in *Sox9* mutants. But in light of the *Gata3* mutant phenotype it is likely that the missing attachment of *Sox9*-mutant placodes to the hindbrain is not the primary reason for the block of placode invagination and subsequent otic vesicle formation. This idea is further supported by our finding that in *Sox9* mosaic embryos, groups of Sox9-positive cells invaginate and form micro-vesicles without any contact to the hindbrain.

Our analysis of *Sox9* mosaic embryos shows that Sox9 is cell-autonomously required for invagination of early placodal cells. The observation that invaginating micro-vesicles are exclusively composed of Sox9-positive cells suggests that Sox9-positive and Sox9-negative cells sort out from one another. A similar segregation of Sox9-positive and negative cells has also been observed during chondrogenesis in chimaeric embryos consisting of $Sox9^{-/-}$ and $Sox9^{+/-}$ cells. In these embryos, $Sox9^{-/-}$ and $Sox9^{+/-}$ cells were intermingled in the early skeletogenic mesenchyme, but Sox9-deficient cells were then excluded form mesenchymal condensations and cartilage primordia (Bi et al., 1999). Such a sorting-out behavior would be expected if *Sox9* controls the adhesive properties of cells. Consistent with such a function, transmission electron microscopic pictures of *Sox9*-mutant otic placodes revealed reduced cell–cell contacts. These changes in epithelial organization are detected more than 12 h before the onset of apoptosis in mutant placodes, and are therefore not a consequence of epithelial cell death. Since the adhesive properties of cells are important for epithelial morphogenesis (Pilot and Lecuit, 2005) it is possible that the failure of otic vesicle formation is a consequence of reduced adhesion between otic placode cells in *Sox9* mutants.

In light of the observed changes in cell–cell contacts and the sorting of Sox9-positive and negative cells in mosaic placodes, the downregulation of EphA4 protein expression in *Sox9* mutants is of particular interest. Members of the Eph receptor tyrosin kinase family and their membrane-tethered ligands, the ephrins, have key roles in the regulation of cell adhesion and cell migration during development (Klein, 2004; Poliakov et al., 2004). In the hindbrain, complementary expression of Epha4 and ephrinB ligands and bi-directional signaling at the interface is thought to control rhombomere-specific cell sorting and the establishment of sharp boundaries between cell populations that do not intermingle (Cooke and Moens, 2002; Xu et al., 1999). In addition, Eph/ephrin signaling has also been implicated in the regulation of cell segregation during somitogenesis and skeletogenesis (Durbin et al., 1998, 2000; Compagni et al., 2003; Davy et al., 2004). It is therefore possible that Eph/ephrin signaling also regulates the segregation of placode precursor cells from non-placode cells, and cell–cell adhesion during otic placode morphogenesis, with Sox9 as an upstream regulator. *Epha4* mutant mice have been generated but have no inner ear defects (Dottori et al., 1998; Helmbacher et al., 2000). However, this is not surprising, since Eph receptor functions are often redundant due to overlapping expression patterns of

several family members and promiscuous binding affinities towards ephrin ligands. Loss of function studies in single genes have likewise so far not revealed a role of Eph/ephrin signaling in somite or hindbrain segmentation (Klein, 2004; Poliakov et al., 2004). It will therefore be important to clarify which other members of the Eph family and which of the ephrin ligands are expressed during inner ear development and how their expression is affected by the absence of Sox9.

In addition, although the EM pictures and laminin stainings show no difference in the basement membrane of control and *Sox9*-mutant placodes, we can not exclude that loss of Sox9 also affects the composition of the extra-cellular matrix on the basal side of the placode, and this could indirectly affect the adhesive properties of the placodal cells. Such a function of Sox9 in regulating the extra-cellular matrix is well established for chondrogenesis. There, Sox9 regulates the expression of extracellular matrix components such as type II collagen (de Crombrugghe et al., 2000; Lefebvre et al., 1997), and Col2a1 is also down-regulated in the *Sox9*-mutant otic placodes, although no defects for in inner ear development have been reported for *Col2a1* knock out mice (Li et al., 1995).

Sox9 mutant placode cells undergo apoptosis

Around E9.0, about 12 h after the first changes in the morphogenetic behavior of *Sox9*-mutant placodes can be seen, the non-invaginated placodal cells of *Sox9* mutants start to be eliminated by apoptosis. Apoptosis of misplaced cells is a frequent phenomenon in development. It is therefore very likely that the observed cell death is an indirect consequence of the changes in epithelial organization or the failure of placode invagination. However, a direct role of Sox9 in promoting cell survival in the otic placode can not be excluded. Previous studies in avian embryos addressing otic placode commitment showed that placodes transplanted to the trunk region survived far away from the hindbrain, whether they formed an otic vesicle or not (Groves and Bronner-Fraser, 2000). It is thus unlikely that an increased distance of the placode from a source of survival signals in the hindbrain is responsible for the observed apoptosis.

Apoptosis has also been reported after inactivation of *Sox9* in trunk neural crest cells and limb mesoderm (Akiyama et al., 2002; Cheung et al., 2005). But also in these tissues, it is unclear whether Sox9 has a direct and cell autonomous effect as a survival factor or if apoptosis is an indirect consequence of other defects.

Species-specific requirement of Sox9 in otic development

In *Xenopus*, depletion of Sox9 protein using morpholino antisense oligonucleotides causes the loss of early otic placode markers and prevents the formation of an otic vesicle (Saint-Germain et al., 2004). This study suggests that Sox9 has a role in the initial specification of the otic placode. In *sox9a*- and *sox9b*-compromised zebrafish, otic vesicles are missing or reduced to vestiges, and Pax2 is not expressed in the otic region. A detailed analysis of the phenotype, however, was not performed, so that it is unclear whether otic placode specification, or subsequent placode morphogenesis and survival is affected (Liu et al., 2003; Yan et al., 2005). In contrast, the formation of a morphologically distinct placode and the normal expression of markers of otic placode specification (*Pax2*, *Pax8,* and *Dlx5*) and of FGF signaling *(Pea3* and *Erm)* in our *Sox9* mutants demonstrate that the specification of the otic placodes in the mouse does not require Sox9. Thus, there appear to be species-specific differences in the requirement for Sox9 in inner ear development between *Xenopus* and mouse. These differences correlate with differences in the timing of the onset of *Sox9* expression: In *Xenopus* and also zebrafish, *Sox9* expression in the presumptive otic placode already starts during neurulation (Liu et al., 2003; Saint-Germain et al., 2004), whereas in the mouse Sox9 protein can first be detected at the 5-somite stage. Our results furthermore exclude that *Sox8* and *Sox10,* the two other members of the SoxE group of the Sox gene family, substitute for mouse *Sox9* in otic specification. Both genes have been shown to be expressed during mouse otic development (Britsch et al., 2001; Sock et al., 2001; Watanabe et al., 2000) and recent studies in *Xenopus* have shown that misexpression of either *Sox9* or *Sox10* results in the formation of enlarged or ectopic otocysts, demonstrating that both factors are equally potent to promote inner ear formation (Taylor and Labonne, 2005). However, we show that expression of both genes starts only after otic placode specification, and that there is a cross regulation between *Sox9* and *Sox10* in mice such that *Sox10* is not expressed in Sox9-deficient otic placodes. Therefore, if *Sox9* has any function in the formation of the otic placode in the mouse, then redundant pathways involving genes other than *SoxE* genes must exist.

In summary, our analysis reveals an important novel role of Sox9 in controlling otic placode invagination in the mouse. In a recent study on the transcriptional control of *Sox9* expression, we have identified an enhancer element conserved between human, mouse and pufferfish, which mediates *Sox9* expression in the inner ear (Bagheri-Fam et al., 2006). Characterization of the transcription factors activating this otic enhancer on the one hand, and identification of the transcriptional targets of Sox9 in the murine otic placode on the other hand, may both contribute to a better understanding of the molecular regulation of otic placode invagination.

Acknowledgments

We thank Gunther Neuhaus for helpful advice and comments concerning electron microscopy, Jean Hebert for providing the *Foxg1*^{Cre} line, Meinrad Busslinger, Francois Guillemot, Tetsuji Mori, Michael Wegner, John Rubenstein, Virginia Papaioannou, and Charlotte A. Peterson for providing plasmids, Michael Wegner for a gift of the Sox9 antibody, Jürgen Zimmer and Johannes vom Berg for help with mouse husbandry, and Roswitha Koppa and Raffaele de Lucca for technical assistance. We are grateful to Elisa McGowan and Soojin Ryu for critical reading of the manuscript. This work was supported by grants from the Deutsche Forschungsgemeinschaft to G.S. (Sche 194/15-3) and to A.N. (SFB592, TP-A12 and GRK1104).

Appendix A. Supplementary data

Supplementary data associated with this article can be found, in the online version, at doi:10.1016/j.ydbio.2008.02.011.

References

Akiyama, H., Chaboissier, M.C., Martin, J.F., Schedl, A., de Crombrugghe, B., 2002. The transcription factor Sox9 has essential roles in successive steps of the chondrocyte differentiation pathway and is required for expression of Sox5 and Sox6. Genes Dev. 16, 2813–2828.

Bagheri-Fam, S., Barrionuevo, F., Dohrmann, U., Gunther, T., Schule, R., Kemler, R., Mallo, M., Kanzler, B., Scherer, G., 2006. Long-range upstream and downstream enhancers control distinct subsets of the complex spatiotemporal Sox9 expression pattern. Dev. Biol. 291, 382–397.

Barald, K.F., Kelley, M.W., 2004. From placode to polarization: new tunes in inner ear development. Development 131, 4119–4130.

Barrionuevo, F., Bagheri-Fam, S., Klattig, J., Kist, R., Taketo, M.M., Englert, C., Scherer, G., 2006. Homozygous inactivation of Sox9 causes complete XY sex reversal in mice. Biol. Reprod. 74, 195–201.

Bi, W., Deng, J.M., Zhang, Z., Behringer, R.R., de Crombrugghe, B., 1999. Sox9 is required for cartilage formation. Nat. Genet. 22, 85–89.

Britsch, S., Goerich, D.E., Riethmacher, D., Peirano, R.I., Rossner, M., Nave, K.A., Birchmeier, C., Wegner, M., 2001. The transcription factor Sox10 is a key regulator of peripheral glial development. Genes Dev. 15, 66–78.

Chaboissier, M.C., Kobayashi, A., Vidal, V.I., Lutzkendorf, S., van de Kant, H.J., Wegner, M., de Rooij, D.G., Behringer, R.R., Schedl, A., 2004. Functional analysis of Sox8 and Sox9 during sex determination in the mouse. Development 131, 1891–1901.

Chapman, D.L., Garvey, N., Hancock, S., Alexiou, M., Agulnik, S.I., Gibson-Brown, J.J., Cebra-Thomas, J., Bollag, R.J., Silver, L.M., Papaioannou, V.E., 1996. Expression of the T-box family genes. Tbx1–Tbx5, during early mouse development. Dev. Dyn. 206, 379–390.

Cheung, M., Chaboissier, M.C., Mynett, A., Hirst, E., Schedl, A., Briscoe, J., 2005. The transcriptional control of trunk neural crest induction, survival, and delamination. Dev. Cell. 8, 179–192.

Compagni, A., Logan, M., Klein, R., Adams, R.H., 2003. Control of skeletal patterning by ephrinB1-EphB interactions. Dev. Cell. 5, 217–230.

Cooke, J.E., Moens, C.B., 2002. Boundary formation in the hindbrain: Eph only it were simple. Trends Neurosci. 25, 260–267.

Davy, A., Aubin, J., Soriano, P., 2004. Ephrin-B1 forward and reverse signaling are required during mouse development. Genes Dev. 18, 572–583.

de Crombrugghe, B., Lefebvre, V., Behringer, R.R., Bi, W., Murakami, S., Huang, W., 2000. Transcriptional mechanisms of chondrocyte differentiation. Matrix Biol. 19, 389–394.

Dorfler, P., Busslinger, M., 1996. C-terminal activating and inhibitory domains determine the transactivation potential of BSAP (Pax-5), Pax-2 and Pax-8. Embo J. 15, 1971–1982.

Dottori, M., Hartley, L., Galea, M., Paxinos, G., Polizzotto, M., Kilpatrick, T., Bartlett, P.F., Murphy, M., Kontgen, F., Boyd, A.W., 1998. EphA4 (Sek1) receptor tyrosine kinase is required for the development of the corticospinal tract. Proc. Natl Acad. Sci. USA 95, 13248–13253.

Durbin, L., Brennan, C., Shiomi, K., Cooke, J., Barrios, A., Shanmugalingam, S., Guthrie, B., Lindberg, R., Holder, N., 1998. Eph signaling is required for segmentation and differentiation of the somites. Genes Dev. 12, 3096–3109.

Durbin, L., Sordino, P., Barrios, A., Gering, M., Thisse, B., Brennan, C., Green, A., Wilson, S., Holder, N., 2000. Anteroposterior patterning is required within segments for somite boundary formation in developing zebrafish. Development 127, 1703–1713.

Firnberg, N., Neubuser, A., 2002. FGF signaling regulates expression of Tbx2, Erm, Pea3, and Pax3 in the early nasal region. Dev. Biol. 247, 237–250.

Gradwohl, G., Dierich, A., LeMeur, M., Guillemot, F., 2000. neurogenin3 is required for the development of the four endocrine cell lineages of the pancreas. Proc. Natl Acad. Sci. U S A 97, 1607–1611.

Groves, A.K., Bronner-Fraser, M., 2000. Competence, specification and commitment in otic placode induction. Development 127, 3489–3499.

Hebert, J.M., McConnell, S.K., 2000. Targeting of cre to the Foxg1 (BF-1) locus mediates loxP recombination in the telencephalon and other developing head structures. Dev. Biol. 222, 296–306.

Helmbacher, F., Schneider-Maunoury, S., Topilko, P., Tiret, L., Charnay, P., 2000. Targeting of the EphA4 tyrosine kinase receptor affects dorsal/ventral pathfinding of limb motor axons. Development 127, 3313–3324.

Henrique, D., Adam, J., Myat, A., Chitnis, A., Lewis, J., Ish-Horowicz, D., 1995. Expression of a Delta homologue in prospective neurons in the chick. Nature 375, 787–790.

Hilfer, S.R., Esteves, R.A., Sanzo, J.F., 1989. Invagination of the otic placode: normal development and experimental manipulation. J. Exp. Zool. 251, 253–264.

Houston, C.S., Opitz, J.M., Spranger, J.W., Macpherson, R.I., Reed, M.H., Gilbert, E.F., Herrmann, J., Schinzel, A., 1983. The campomelic syndrome: review, report of 17 cases, and follow-up on the currently 17-year-old boy first reported by Maroteaux et al in 1971. Am J Med Genet 15, 3–28.

Kiernan, A.E., Steel, K.P., Fekete, D.M., 2002. Development of the mouse inner ear. In: Rossant, J., Tam, P.P.L. (Eds.), Mouse Development. Patterning Morphogenesis, and Organogenesis. Academic Press, pp. 539–566.

Kist, R., Schrewe, H., Balling, R., Scherer, G., 2002. Conditional inactivation of Sox9: a mouse model for campomelic dysplasia. Genesis 32, 121–123.

Klein, R., 2004. Eph/ephrin signaling in morphogenesis, neural development and plasticity. Curr. Opin. Cell. Biol. 16, 580–589.

Kuhlbrodt, K., Herbarth, B., Sock, E., Hermans-Borgmeyer, I., Wegner, M., 1998. Sox10, a novel transcriptional modulator in glial cells. J. Neurosci. 18, 237–250.

Ladher, R.K., Anakwe, K.U., Gurney, A.L., Schoenwolf, G.C., Francis-West, P.H., 2000. Identification of synergistic signals initiating inner ear development. Science 290, 1965–1967.

Ladher, R.K., Wright, T.J., Moon, A.M., Mansour, S.L., Schoenwolf, G.C., 2005. FGF8 initiates inner ear induction in chick and mouse. Genes Dev. 19, 603–613.

Lecureuil, C., Fontaine, I., Crepieux, P., Guillou, F., 2002. Sertoli and granulosa cell-specific Cre recombinase activity in transgenic mice. Genesis 33, 114–118.

Lefebvre, V., Huang, W., Harley, V.R., Goodfellow, P.N., de Crombrugghe, B., 1997. SOX9 is a potent activator of the chondrocyte-specific enhancer of the pro alpha1(II) collagen gene. Mol. Cell Biol. 17, 2336–2346.

Li, S.-W., Prockop, D.J., Helminen, H., Fässler, R., Lapveteläinen, T., Kiraly, K., Peltarri, A., Arokoski, J., Lui, H., Arita, M., Khillan, J.S., 1995. Transgenic mice with targeted inactivation of the Col2a1 gene develop a skeleton with membranous and periosteal bone but no endochondral bone. Genes Dev. 9, 2821–2830.

Lillevali, K., Haugas, M., Matilainen, T., Pussinen, C., Karis, A., Salminen, M., 2006. Gata3 is required for early morphogenesis and Fgf10 expression during otic development. Mech. Dev. 123, 415–429.

Liu, J.K., Ghattas, I., Liu, S., Chen, S., Rubenstein, J.L., 1997. Dlx genes encode DNA-binding proteins that are expressed in an overlapping and sequential pattern during basal ganglia differentiation. Dev. Dyn. 210, 498–512.

Liu, D., Chu, H., Maves, L., Yan, Y.L., Morcos, P.A., Postlethwait, J.H., Westerfield, M., 2003. Fgf3 and Fgf8 dependent and independent transcription factors are required for otic placode specification. Development 130, 2213–2224.

Mansour, S.L., Martin, G.R., 1988. Four classes of mRNA are expressed from the mouse int-2 gene, a member of the FGF gene family. Embo J. 7, 2035–2041.

Means, A.L., Chytil, A., Moses, H.L., Coffey Jr., R.J., Wright, C.V., Taketo, M.M., Grady, W.M., 2005. Keratin 19 gene drives Cre recombinase expression throughout the early postimplantation mouse embryo. Genesis 42, 23–27.

Mori, T., Wanaka, A., Taguchi, A., Matsumoto, K., Tohyama, M., 1995. Differential expressions of the eph family of receptor tyrosine kinase genes (sek, elk, eck) in the developing nervous system of the mouse. Brain Res. Mol. Brain Res. 29, 325–335.

Moro-Balbas, J.A., Gato, A., Alonso, M.I., Martin, P., de la Mano, A., 2000. Basal lamina heparan sulphate proteoglycan is involved in otic placode invagination in chick embryos. Anat. Embryol. (Berl) 202, 333–343.

Nagy, A., Gertsenstein, M., Vintersten, K., Behringer, R., 2003. Manipulating the Mouse Embryo: A Laboratory Manual. Cold Spring Harbor Laboratory Press, Cold Spring Harbor, New York.

Noramly, S., Grainger, R.M., 2002. Determination of the embryonic inner ear. J. Neurobiol. 53, 100–128.

Ohyama, T., Mohamed, O.A., Taketo, M.M., Dufort, D., Groves, A.K., 2006. Wnt signals mediate a fate decision between otic placode and epidermis. Development 133, 865–875.

Phillips, B.T., Bolding, K., Riley, B.B., 2001. Zebrafish fgf3 and fgf8 encode redundant functions required for otic placode induction. Dev. Biol. 235, 351–365.

Phillips, B.T., Storch, E.M., Lekven, A.C., Riley, B.B., 2004. A direct role for Fgf but not Wnt in otic placode induction. Development 131, 923–931.

Pilot, F., Lecuit, T., 2005. Compartmentalized morphogenesis in epithelia: from cell to tissue shape. Dev. Dyn. 232, 685–694.

Pirvola, U., Ylikoski, J., Trokovic, R., Hebert, J.M., McConnell, S.K., Partanen, J., 2002. FGFR1 is required for the development of the auditory sensory epithelium. Neuron 35, 671–680.

Poliakov, A., Cotrina, M., Wilkinson, D.G., 2004. Diverse roles of eph receptors and ephrins in the regulation of cell migration and tissue assembly. Dev. Cell. 7, 465–480.

Rahkonen, O., Savontaus, M., Abdelwahid, E., Vuorio, E., Jokinen, E., 2003. Expression patterns of cartilage collagens and Sox9 during mouse heart development. Histochem. Cell. Biol. 120, 103–110.

Raible, F., Brand, M., 2001. Tight transcriptional control of the ETS domain factors Erm and Pea3 by Fgf signaling during early zebrafish development. Mech. Dev. 107, 105–117.

Roehl, H., Nusslein-Volhard, C., 2001. Zebrafish pea3 and erm are general targets of FGF8 signaling. Curr. Biol. 11, 503–507.

Saint-Germain, N., Lee, Y.H., Zhang, Y., Sargent, T.D., Saint-Jeannet, J.P., 2004. Specification of the otic placode depends on Sox9 function in Xenopus. Development 131, 1755–1763.

Sock, E., Schmidt, K., Hermanns-Borgmeyer, I., Bosl, M.R., Wegner, M., 2001. Idiopathic weight reduction in mice deficient in the high-mobility-group transcription factor Sox8. Mol. Cell. Biol. 21, 6951–6959.

Stolt, C.C., Lommes, P., Sock, E., Chaboissier, M.C., Schedl, A., Wegner, M., 2003. The Sox9 transcription factor determines glial fate choice in the developing spinal cord. Genes Dev. 17, 1677–1689.

Stolt, C.C., Lommes, P., Friedrich, R.P., Wegner, M., 2004. Transcription factors Sox8 and Sox10 perform non-equivalent roles during oligodendrocyte development despite functional redundancy. Development 131, 2349–2358.

Taylor, K.M., Labonne, C., 2005. SoxE factors function equivalently during neural crest and inner ear development and their activity is regulated by SUMOylation. Dev. Cell. 9, 593–603.

Taylor, J.M., Dupont-Versteegden, E.E., Davies, J.D., Hassell, J.A., Houle, J.D., Gurley, C.M., Peterson, C.A., 1997. A role for the ETS domain transcription factor PEA3 in myogenic differentiation. Mol. Cell. Biol. 17, 5550–5558.

Tokita, N., Chandra-Sekhar, H.K., Daly, J.F., Becker, M.H., Aleksic, S., 1979. The Campomelic syndrome. Temporal bone histopathologic features and otolaryngologic manifestations. Arch. Otolaryngol. 105, 449–454.

Visconti, R.P., Hilfer, S.R., 2002. Perturbation of extracellular matrix prevents association of the otic primordium with the posterior rhombencephalon and inhibits subsequent invagination. Dev. Dyn. 223, 48–58.

Watanabe, K., Takeda, K., Katori, Y., Ikeda, K., Oshima, T., Yasumoto, K., Saito, H., Takasaka, T., Shibahara, S., 2000. Expression of the Sox10 gene during mouse inner ear development. Brain Res. Mol. Brain Res. 84, 141–145.

Wright, T.J., Mansour, S.L., 2003a. Fgf3 and Fgf10 are required for mouse otic placode induction. Development 130, 3379–3390.

Wright, T.J., Mansour, S.L., 2003b. FGF signaling in ear development and innervation. Curr. Top. Dev. Biol. 57, 225–259.

Xu, Q., Mellitzer, G., Robinson, V., Wilkinson, D.G., 1999. In vivo cell sorting in complementary segmental domains mediated by Eph receptors and ephrins. Nature 399, 267–271.

Yan, Y.L., Willoughby, J., Liu, D., Crump, J.G., Wilson, C., Miller, C.T., Singer, A., Kimmel, C., Westerfield, M., Postlethwait, J.H., 2005. A pair of Sox: distinct and overlapping functions of zebrafish sox9 co-orthologs in craniofacial and pectoral fin development. Development 132, 1069–1083.